



Highly sensitive measurements of ^{222}Rn permeability in Au

S.K. Bhattacharyya, S.K. Pabi *

Metallurgical and Materials Engineering Department, Indian Institute of Technology, Kharagpur 721 302, India

Received 27 September 1996; accepted 9 December 1996

Abstract

The permeation rate of ^{222}Rn (N_{Rn}) through the high purity annealed and cold worked Au was measured at 30–150°C on atomic scale by means of a modified highly sensitive α -spectroscopic method. Virgin annealed Au was impermeable to ^{222}Rn upto 150°C, but it became permeable after being subjected to a thermal cycle of negative magnitude, whereas virgin cold worked Au was highly permeable at room temperature. Prolonged isothermal holding resulted in permeation plateaux in annealed Au, and fairly well defined permeation peaks in cold worked Au. The activation energy of permeation in cold worked Au (18.0 to 22.5 kJ/mol) was appreciably smaller than that in annealed Au (33.2 to 35.4 kJ/mol), while in the former N_{Rn} was about two orders of magnitude higher. The observations have been interpreted in terms of capture of vacancies by diffusing ^{222}Rn atoms and structural changes in diffusion paths (e.g., grain boundaries) by deformation induced defects.

1. Introduction

Extensive studies on gas permeation in materials mostly deal with hydrogen permeation due to the relative ease of measurements and importance of the topic in structural embrittlement [1–5]. Permeability at low partial pressure is, however, not well understood, and even for the same material the permeability can differ by several orders of magnitude at a given temperature [1]. This divergence is believed to be mainly related to the surface processes and the characteristics of the trapping centres present in the materials [1–4]. Studies on the permeation of He has also drawn considerable attention in recent years due to the problem of He embrittlement of fusion reactors' structural components, which occurs by intergranular bubble formation [6–10]. The permeation flux of inert gases in metals is usually very small, because the inert gases are almost insoluble in metals [11,12] due to their large size [13]. Studies on radon permeation/diffusion are relatively few in number. Matzke et al. [14] studied the Rn diffusion in cold worked Ag by the high energy ion bombardment technique, while Legoux and Merini [15] measured the

diffusivity of Rn in Ta by nuclear recoil. Both these methods measure transient diffusivity in the presence of radiation induced defects. Pabi and Hahn [16] developed a highly sensitive α -spectroscopic method for measuring ^{222}Rn permeability on atomic scale ($\sim 10^4$ atoms/m² s). The method is able to track the ^{222}Rn permeability in a material over a long period of time (e.g., months). They have found that ^{222}Rn dissolves in polycrystalline Au, and its permeability in Au varies with the thermal history of the specimen at low homologous temperatures, T_{H} (≤ 0.27). However, they did not report any value for the activation energy of ^{222}Rn permeation (Q_{p}) in Au at different stages of the process. Recently, Bhattacharyya and Pabi [17] have studied the ^{222}Rn permeability in Pb at higher T_{H} (≥ 0.68) using a modified version of the earlier α -spectroscopic method [16]. The investigation has revealed that permeability of ^{222}Rn in Pb at high T_{H} (≥ 0.68) also depends strongly on the thermal schedule in the course of permeation. They have found that ^{222}Rn permeability in Pb gradually increases to a plateau during prolonged isothermal holding (> 135 h). The permeation takes place with an unusually low magnitude of Q_{p} (≈ 8.2 kJ/mol), possibly indicating that ^{222}Rn permeates in annealed Pb mainly through the grain boundaries by capturing vacancies.

* Corresponding author. Tel.: +91-3222 55 221, ext. 4764; fax: +91-3222 55 303; e.mail: skpabi@hijli.iitkgp.ernet.in.

In case of permeation through Pb, it may be argued that the strong dependence of ^{222}Rn permeability on the thermal history in the course of permeation may be due to the formation of surface layers (e.g., oxides) on Pb. However, the same argument would not hold well in case of Au. Permeation of a monatomic gas like ^{222}Rn in a noble metal like Au represents an ideal condition, where dissociation and recombination of permeating atoms at the specimen surfaces are not involved, and the possibility of formation of any surface oxide layer on specimen is excluded. Structural imperfections produced by deformation of the specimen can also influence the permeation characteristics [18–20]. The present paper reports for the first time a systematic study of ^{222}Rn permeability in annealed and cold worked Au at low T_H (0.23 to 0.32) over an extended period of time. Since the present experimental method enables the measurement of ^{222}Rn flux almost atom by atom, several new characteristic features of the permeation have been revealed.

2. Experimental

A high purity Au (99.995%) sheet of 1.5 mm thickness, received from Nuclear Fuel Complex, India, was cross rolled with intermediate annealing at 700°C to produce foils of $\sim 26 \mu\text{m}$ thickness with a final deformation of 38%. A portion of the foil was annealed at 700°C for 1 h. The foils were washed thoroughly in acetone and benzene

before using them as specimen for the permeability measurements. For metallographic examination, a piece of the annealed and cold worked foil was electropolished (12 V, 65°C) in an electrolyte containing 15 g chromic oxide, 75 ml acetic acid and 3 ml distilled water, using a platinum cathode. The average grain size of the foils was measured by the standard intercept method [21].

Fig. 1 shows schematically the modified α -spectroscopic method used for measuring ^{222}Rn permeability. Its description, working principle along with its mathematical model have been given earlier [16,17]. In its essence, a ^{226}Ra needle of 0.5 mCi activity serves as a practically infinite source of ^{222}Rn atoms [16,22,23] which permeate through the foils under investigation and accumulate in a metallic collection chamber (MCC), where they decay to ^{218}Po ions. The ^{222}Rn permeation flux (N_{Rn}) through the specimen is estimated through the following relation [16] using the α -decay counting rate (I_S) of ^{218}Po that has been collected on the surface barrier α -detector by application of an electrostatic field:

$$N_{\text{Rn}} = (dI_S/dt)/(fGA\lambda_{\text{Rn}}); \quad kt \ll 1, \quad (1)$$

where the geometric efficiency of the detector $G = 0.5$ for a 4π emission, A is the area of the foil available for permeation, and λ_{Rn} is the decay constant of ^{222}Rn ($2.1 \times 10^{-6} \text{ s}^{-1}$). f and k are the net collection efficiency (0.192) and effective decay constant ($2.3 \times 10^{-6} \text{ s}^{-1}$), respectively, which have been estimated in a manner outlined earlier [17].

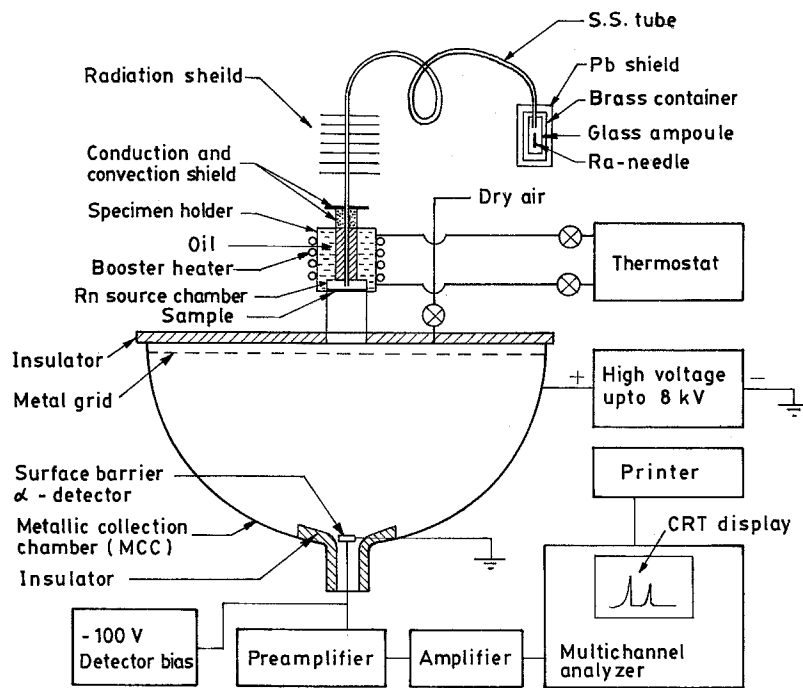


Fig. 1. Schematic illustration of the ^{222}Rn permeation measuring equipment.

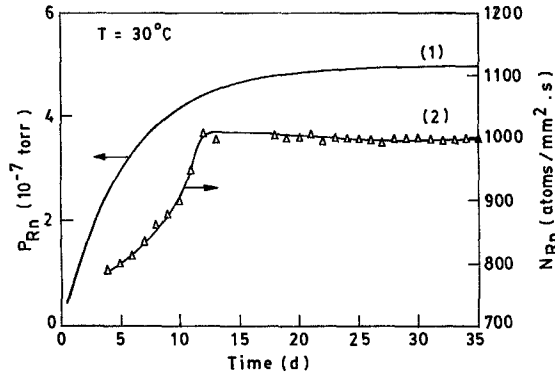


Fig. 2. (1) Partial pressure P_{Rn} of ^{222}Rn in the specimen chamber, and (2) permeation rate N_{Rn} in cold worked Au, as a function of isothermal holding time at room temperature (30°C) in the preparatory period.

Mathematical analysis of the measuring method took into account any possible loss of ^{222}Rn , caused by its decay within the foil, as well as due to its adsorption by and leakage from the MCC [16]. The analysis evolved the guidelines for quantitative measurement of N_{Rn} on atomic scale. By modifying the design of the electrostatic collector and specimen holder, the present method can measure the ^{222}Rn flux down to the order of $5000 \text{ atoms}/\text{m}^2 \text{ s}$ over a wider temperature range with better control over the process variables [17].

In the present experiments, the ^{226}Ra needle was sealed in the specimen chamber using the foil specimen as the window. The specimen holder was then held at room temperature (30°C) for 35 d to achieve a steady state concentration or partial pressure ($\sim 5 \times 10^{-7} \text{ torr}$) of radon inside the specimen chamber (Fig. 2) [16,17]. During this 'preparatory period' the specimen chamber was kept coupled with the MCC of the permeation measuring equipment (Fig. 1) to detect any permeation flux through the foil. Subsequently, permeation measurements were carried out at various temperatures, T_p ($\leq 150^\circ\text{C}$), controlled to $\pm 0.05^\circ\text{C}$.

3. Results

Measurements on the polished foil surface yielded an average grain size of $58 \mu\text{m}$ in the cross rolled Au, while in the annealed (700°C , 1 h) recrystallized sample it was $42 \mu\text{m}$. These sizes are considerably larger than the foil thickness ($26 \mu\text{m}$). Hence, most of the grain boundaries are expected to be almost in the transverse direction to the foil surface.

Since the permeability in Au is known to depend on the thermal history of the specimen [16], the heat treatment schedule of the annealed and cold worked Au is displayed in Fig. 3a and b, respectively. Here, h_{6A} , h_{8A} (Fig. 3a),

h_{2W} , h_{4W} , and h_{6W} (Fig. 3b) represent step-heating experiments of short duration ($\sim 12 \text{ h}$), while h_{1A} , h_{2A} , h_{3A} , h_{5A} , h_{7A} , h_{9A} (Fig. 3a), h_{1W} , h_{3W} , h_{5W} , and h_{7W} (Fig. 3b) are prolonged ($\geq 108 \text{ h}$) isothermal holding treatments, and h_{4A} is the schedule for introducing a thermal cycle of negative magnitude (TCNM). The permeation flux (N_{Rn}) recorded in the course of these treatments (except in h_{1W}) is also shown in Fig. 3, and N_{Rn} in h_{1W} is displayed in Fig. 2.

Permeation measurements were carried out at 30 , 50 , 60 , 70 , 80 , 90 , 100 , 110 , 120 , 130 , 140 , and 150°C . Before starting the permeation measurements at any T_p , the MCC was flushed with dry air to remove any residual ^{222}Rn atoms in it. Moreover, flushing was also done at an interval of $45,000 \text{ s}$ in the course of prolonged measurements at any T_p to satisfy the condition $kt \ll 1$ in Eq. (1).

Treatment h_{1A} in Fig. 3a shows that the specimen chamber containing the annealed Au foil was initially held at room temperature (30°C) for 35 d, and during this preparatory period there was no permeation flux through the specimen. Isothermal holding of the annealed foil at 100°C for 14 d (h_{2A}) also did not show any permeation flux on atomic scale. Even after isothermal holding at 150°C for 4.5 d (h_{3A}), the foil remained impermeable to ^{222}Rn atoms. At this stage, the specimen was subjected to a TCNM comprising of cooling ($\sim 5^\circ\text{C}/\text{min}$) to room

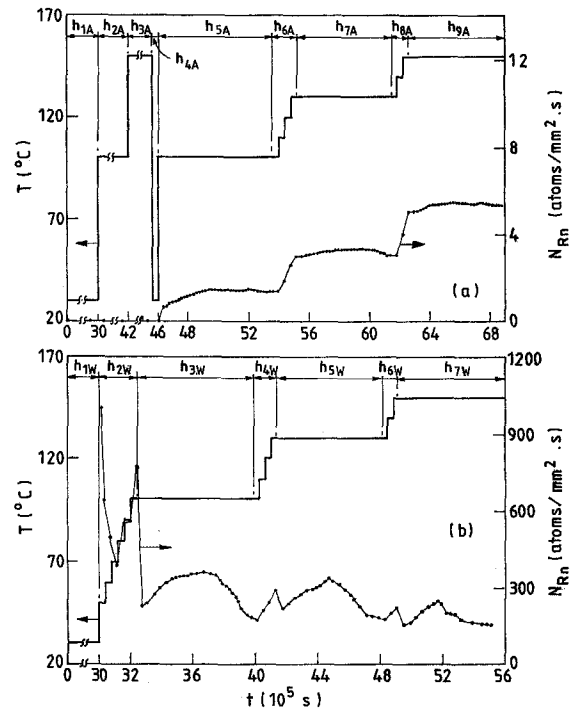


Fig. 3. Thermal schedule of (a) annealed and (b) cold worked Au specimen in the course of permeation. Filled circles show measured N_{Rn} in the course of these treatments except in h_{1W} , which is displayed in Fig. 2.

temperature (30°C) followed by isothermal holding for 12 h and reheating to 100°C (i.e., treatment h_{4A} in Fig. 3a). It was interesting to note that ^{222}Rn started permeating through the annealed specimen. The permeation flux (N_{Rn}) gradually increased with the duration of isothermal holding (t_I) at 100°C in treatment h_{5A} (Fig. 3a) and reached a plateau, $N_{\text{Rn(steady)}}$ after 3.2×10^5 s, while beyond 6.1×10^5 s N_{Rn} showed a very marginal decline (Fig. 4a), possibly due to the contamination of the ^{222}Rn diffusion paths by the daughter products. The step-heating treatment upto 130°C (in h_{6A} , Fig. 3a) introduced at this stage yielded the activation energy of permeation, $Q_{P(tr)} = 33.2 \pm 0.7$ kJ/mol, from an Arrhenius plot of N_{Rn} (Fig. 5a). During subsequent isothermal holding at 130°C in h_{7A} the permeation flux (N_{Rn}) once again attained a plateau (Fig. 4a) in a manner similar to that at 100°C in h_{5A} (Fig. 3a). As expected, $N_{\text{Rn(steady)}}$ at 130°C was higher than that at 100°C (Fig. 4a). Immediately thereafter, the step-heating experiment h_{8A} (Fig. 3a) gave $Q_{P(tr)} = 35.4 \pm 0.3$ kJ/mol (Fig. 5a), which is quite consistent with the results of treatment h_{6A} (Fig. 3a). Fig. 4a shows the course of attainment of $N_{\text{Rn(steady)}}$ during the ensuing isothermal treatment at 150°C in h_{9A} (Fig. 3a). It is interesting to note from Fig. 5a that the Arrhenius plot of $N_{\text{Rn(steady)}}$, obtained during isothermal holding at 100, 130 and 150°C (i.e., in h_{5A} , h_{7A} and h_{9A} of Fig. 3a), yielded $Q_{P(st)} = 34.6 \pm 0.9$ kJ/mol (Fig. 5a), which was also quite close to $Q_{P(tr)}$ determined by step-heating experiments h_{6A} and h_{8A} .

The permeability in cold worked Au showed quite contrasting characteristics, when compared to that in an-

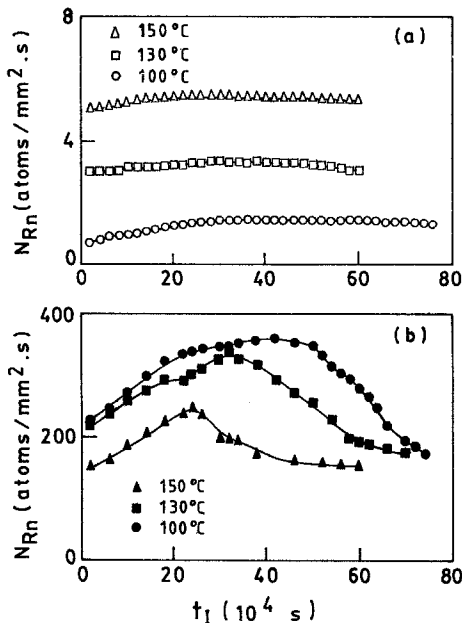


Fig. 4. N_{Rn} versus isothermal holding time t_I for (a) annealed Au in the course of treatment h_{5A} , h_{7A} and h_{9A} , and (b) cold worked Au in treatment h_{3W} , h_{5W} and h_{7W} of Fig. 3 (see text).

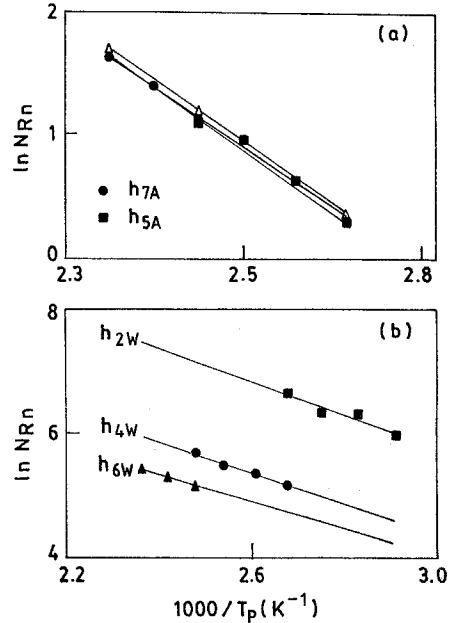


Fig. 5. Plot of N_{Rn} versus $(1000/T_p)$ for (a) annealed and (b) cold worked Au. Filled symbols are for step heating treatments and open symbols correspond to prolonged isothermal holding treatment.

nealed Au. In the cold worked Au specimen the ^{222}Rn permeated at an appreciable rate at room temperature (30°C) right from the start of the preparatory period, i.e., after sealing the ^{226}Ra needle with the foil specimen as the window (Fig. 2). During this period (shown as h_{1W} in Fig. 3b), the partial pressure of ^{222}Rn in the specimen chamber gradually increased to a saturation value (Fig. 2) [16,17] and the permeation flux, N_{Rn} also manifested a concurrent increase to attain a (near) steady level of 1001 atoms/mm² s (Fig. 2). This permeation flux causes a negligible (~1%) reduction in the steady state ^{222}Rn concentration inside the specimen chamber, as estimated through Eq. (1) of Ref. [16]. After the period in h_{1W} (Fig. 3b), the step-heating experiment involving short time (~12 h) isothermal holding at 50, 60, 70, 80, 90, 100°C was carried out in treatment h_{2W} (Fig. 3b). N_{Rn} decreased sharply to 640 atoms/mm² s during holding at 50°C for 12 h (Fig. 3b) and the decline continued during short time (~12 h) holding at 60 and 70°C in h_{2W} (Fig. 3b), possibly indicating the relaxation of some defects introduced by cold working. However, subsequent step-heating at 80, 90 and 100°C in h_{2W} resulted in a gradual increase in N_{Rn} (Fig. 3b). These values of N_{Rn} measured at 70 to 100°C in treatment h_{2W} fall on a straight line in an Arrhenius plot (Fig. 5b), yielding an activation energy $Q_{P(tr)} = 22.5 \pm 0.7$ kJ/mol. During the subsequent isothermal holding of the specimen at 100°C in treatment h_{3W} (Fig. 3b), N_{Rn} dropped drastically from 773 atoms/mm² s to 227 atoms/mm² s between 12 to 24 h, and then it gradually increased to

attain a peak value, $N_{\text{Rn(peak)}} = 360 \text{ atoms/mm}^2 \text{ s}$ at $t_1 \approx 4.2 \times 10^5 \text{ s}$ (Fig. 4b). With further increase in t_1 , N_{Rn} gradually decreased (Fig. 4b) at a rate much faster than that in the course of isothermal holding of annealed Au at the same temperature (Fig. 4a). The ensuing step-heating treatment $h_{4\text{W}}$ (Fig. 3b) yielded $Q_{\text{P(tr)}} = 20.9 \pm 0.5 \text{ kJ/mol}$. Thereafter, the isothermal holding was carried out at 130°C in $h_{5\text{W}}$, and the corresponding N_{Rn} once again dropped sharply between 12–24 h, and then gradually increased to reach $N_{\text{Rn(peak)}} = 336 \text{ atoms/mm}^2 \text{ s}$ in a manner similar to that at 100°C in $h_{3\text{W}}$. The step-heating experiment $h_{6\text{W}}$ immediately after $h_{5\text{W}}$ yielded $Q_{\text{P(tr)}} = 18.0 \pm 0.2 \text{ kJ/mol}$, which is somewhat lower than $Q_{\text{P(tr)}}$ in $h_{2\text{W}}$ or $h_{4\text{W}}$. In the subsequent isothermal treatment at 150°C in $h_{7\text{W}}$ (Fig. 3b) the variation of N_{Rn} followed a trend similar to that at 100 and 130°C in $h_{3\text{W}}$ and $h_{5\text{W}}$ (Fig. 3b), respectively. However, at any given temperature, N_{Rn} in cold worked Au was about two orders of magnitude higher than that in annealed Au, as evidenced by Fig. 3. Fig. 4b shows that in cold worked Au the magnitude of $N_{\text{Rn(peak)}}$ and the time to attain it (t_{peak}) decreased with the increase in T_{p} of prolonged isothermal holding (i.e., treatment $h_{3\text{A}}$, $h_{5\text{A}}$ and $h_{7\text{A}}$ in Fig. 3b).

4. Discussion

Inert gases are almost insoluble in metals [11,12]. For example, the maximum solubility of He in Ni near its melting point is $\sim 10^{-8}$ [24]. The solubility of Kr [25] or Xe [26] is less than 10^{-7} in liquid metals (e.g., Cd, In, Pb, Bi). According to Rimmer and Cottrell [13], the extremely low solubility of fission gases like Kr and Xe in metallic crystal is not because of their lack of cohesion, but because of their large size, and hence such a trend is expected to hold for other fission products with similar radii. The approximate crystalline radius of Rn ($\sim 0.2 \text{ nm}$) [17] is much larger than the radius of Au (0.144 nm) [27]. Present work, as well as, the earlier results [16] of permeation in Au indicate that ^{222}Rn has some solubility in annealed and cold worked polycrystalline Au at low T_{H} ($0.23\text{--}0.32$). In polycrystalline solids, the grain boundary regions or dislocations are more receptive to larger atoms due to the existence of a wider spectrum of interatomic distances in these regions [28,29]. Therefore, ^{222}Rn atoms are expected to ‘dissolve’ in polycrystalline Au predominantly at such crystal imperfections.

Annealed Au was initially impermeable to ^{222}Rn atoms during prolonged isothermal holding at 30, 100 and 150°C (in $h_{1\text{A}}$ to $h_{3\text{A}}$ of Fig. 3a). But the permeation is triggered after the introduction of a thermal cycle of negative magnitude (TCNM) through treatment $h_{4\text{A}}$ (Fig. 3a). This result cannot be attributed to the rupture of any surface layer during the TCNM, since such a layer (e.g., oxide) does not form on Au. Besides, the possibility of having quenched-in excess (lattice) vacancies at T_{p} may be excluded, since the

magnitude of the thermal pulse is negative. Probably, the lattice strain around ^{222}Rn atoms may play an important role during this TCNM. It is plausible that the large mismatch between the Au and Rn atom might provoke the flow of vacancies towards ^{222}Rn atoms during TCNM, and as a consequence the permeation is initiated.

In case of annealed Au, the $Q_{\text{P(tr)}}$ values measured in the step-heating experiments (i.e., in $h_{6\text{A}}$ and $h_{8\text{A}}$) are almost the same as that of $Q_{\text{P(st)}}$ derived from permeation plateaux in prolonged isothermal holding in $h_{5\text{A}}$, $h_{7\text{A}}$ and $h_{9\text{A}}$ (Fig. 5a). This possibly indicates that the effective mechanism of permeation has not undergone any change in course of the step-heating and prolonged isothermal holding treatments in $h_{5\text{A}}$ to $h_{9\text{A}}$ (Fig. 3a). In this respect the present results of permeation in Au at low homologous temperature ($T_{\text{H}} \leq 0.32$) are quite similar to that in Pb at higher T_{H} (≥ 0.68) [17]. The Arrhenius plots in Fig. 5a evidence that the corresponding pre-exponential factor (P_0), which is related to the number of active permeation sites, is increased by about 44% during prolonged isothermal holding of annealed Au at low T_{H} (≤ 0.32). In contrast, about 29% increase of P_0 was observed in similar experiments with annealed Pb at higher T_{H} (≥ 0.68) [17]. In the present experiments Q_{p} (33.2 to 35.4 kJ/mol) is substantially higher than Q_{p} for Rn permeation in Pb ($\sim 8.2 \text{ kJ/mol}$) [17]. Q_{p} may be considered to be equal to the sum of the activation energies for diffusion (Q_{D}) and dissolution (Q_{S}). The present values of Q_{p} in Au are much smaller than Q_{D} of Rn in cold worked Ag ($\sim 130 \text{ kJ/mol}$) determined by the high energy ion bombardment technique [14], but it is higher than Q_{D} of Rn in Ta ($\sim 8 \text{ kJ/mol}$) determined by nuclear recoil experiments [15]. It may be pointed out that both nuclear recoil and ion bombardment experiments represent transient states of diffusion, but in the former the broad energy spectrum of fission recoil causes difficulties in controlling the damage during exposure, while the high energy ion bombardment technique permits a more detailed study of the influence of surface proximity and defects created during bombardment [30]. On the other hand, the present experiments record the time modulation of permeability over an extended period of time (cf. Fig. 3), and there is no externally impressed force to cause ionization of Rn atoms during its incorporation in the metal lattice. It is interesting to note that the present Q_{p} values in annealed Au (33.2 to 35.4 kJ/mol) are much smaller than the lattice self diffusion energy in Au (176.6 kJ/mol) [31] or the grain boundary self diffusion energy, $Q_{\text{D(g,b)}}$ of Au (84 kJ/mol) [32]. It is known that noble gases like Kr and Xe have lower values of Q_{D} in annealed Ag (142 and 157.5 kJ/mol, respectively) [33,34] as compared to that for volume self diffusion in Ag (192.3 kJ/mol) [35,36]. In the present experiments, the very small magnitude of the permeation flux ($\approx 0.7 \text{ atoms/mm}^2 \text{ s}$) and Q_{p} (33.2 to 35.4 kJ/mol) apparently indicate that ^{222}Rn permeates in annealed Au mainly through some special sites of the specimen, e.g., grain

boundaries or grain boundary triple junctions. Since the volume of a neutral Rn atom is ~ 3 times the volume of an Au-ion [17,27], the contribution of lattice dislocations to Rn permeation is expected to be marginal. LeClaire et al. [37] have found that Ar diffuses in Ag by a vacancy mechanism. In fact, the very low activation energy of fission gases in uranium has also been attributed by Rimmer and Cottrell [13] to the ability of these gas atoms to capture vacancies and diffuse through the grain boundaries. It may, therefore, be postulated that ^{222}Rn atoms permeate through Au by a similar mechanism and enhance the free volume in the grain boundaries in the course of permeation. The plateaux during isothermal holding experiments h_{5A} , h_{7A} and h_{9A} possibly signify a dynamic equilibrium between the capture and release of such vacancies by the permeating ^{222}Rn atoms [17].

While annealed Au was impermeable to ^{222}Rn during the preparatory period at room temperature (30°C) in treatment h_{1A} (Fig. 3a), the cold worked Au at this stage (i.e., in h_{1W} of Fig. 3b) manifested appreciable permeability (Fig. 2), possibly due to the large population of crystal defects introduced by prior plastic deformation. Matzke et al. [14] have reported earlier that in the bombardment energy range of 3–85 keV the dislocations induced by cold working enhance the inert gas (Kr, Xe, Rn) diffusion in Ag by several orders of magnitude, as compared to that in annealed sample. However, Rickers and Sorenson [30] could not find a similar effect for Kr and Xe diffusion in cold worked Cu by the high energy (20–450 keV) ion bombardment technique. Perhaps in the latter case the defects created during high energy ion bombardment mask the influence of deformation induced defects on the diffusivity.

In the present study, the $Q_{P(tr)}$ values for cold worked Au (18.0 to 22.5 kJ/mol) are appreciably smaller than those in the annealed sample (33.2 to 35.4 kJ/mol). Reduction in Q_D for Kr and Xe diffusion in cold worked Ag (~ 130 kJ/mol) compared to that in annealed Ag (~ 169 kJ/mol) has also been reported earlier [14,38]. However, as compared to all these Q_D values or $Q_{D(g,b)}$ of Au (84 kJ/mol [32]), the present $Q_{P(tr)}$ values are much smaller, and hence, an interpretation of the effects of cold work in the present experiments has to consider the associated changes in the grain boundary structure. It may be pointed out that the extrinsic boundary dislocations (ledges) introduced into the boundaries by cold working result in nonequilibrium boundary structure and cause an increase in the energy of grain boundaries in plastically deformed metals [39,40]. In addition, such extrinsic dislocations are known to influence other boundary properties such as boundary migration, boundary sliding and grain boundary precipitation, etc. [40]. In the present work the reduction in $Q_{P(tr)}$ in cold worked Au may also originate from similar changes in grain boundary structures.

The sharp drop in permeability of cold worked Au during heating at 50, 60 or 70°C in h_{2W} (Fig. 3b) is

indicative of the relaxation of some deformation induced defects. Moreover, the drop in permeability during the first 12–24 h at higher temperatures (i.e., in h_{3W} , h_{5W} and h_{7W}) may also be attributed to the progress of such relaxation processes. This is also borne out by the Arrhenius plots for the step-heating experiments (h_{2W} , h_{4W} and h_{6W}) in Fig. 5b. It is seen that $Q_{P(tr)}$ decreases marginally from 22.5 to 18.0 kJ/mol at higher step-heating temperatures, and a similar effect has been reported earlier for Pb at higher T_H [17]. However, the calculation from Fig. 5b evidences that the pre-exponential factor (P_0) decreases by about two orders of magnitude in treatment h_{6W} as compared to that in h_{2W} , which indicates that many of the active sites for permeation in h_{2W} become nonfunctional at h_{4W} or h_{6W} . It may be mentioned that in the cluster assembled nanocrystalline Cu containing a large density of grain boundaries, the structural relaxation of grain boundaries during annealing at low T_H (at 100°C for 14 h) causes an appreciable reduction in the interdiffusivity of Bi [41]. The present permeation temperatures ($T_H \leq 0.32$) are also considerably lower than those required for annihilation of lattice dislocations or extrinsic boundary dislocations in the cold worked specimen [40,42]. Hence, the relaxation process in the present cold worked Au is likely to be related to the excess vacancies generated by plastic deformation.

It is interesting to note that prolonged isothermal holding of annealed Au results in a permeation plateau (Fig. 4a), while similar experiments with cold worked Au yield a reasonably well defined peak. The decrease of peak height and time to reach the peak (t_{Peak}) with the increase in T_P bears a similarity with the kinetics of clustering and precipitation in precipitation hardenable alloys, where for the purpose of kinetic data analysis the resistivity or hardness peaks are assumed to correspond to some particular state of the structure [43–49]. Thus, if t_{Peak} in Fig. 4b is also assumed to be related to a particular state of defects or structure relevant to the permeability, an Arrhenius plot of t_{Peak} (from Fig. 4b) in Fig. 6 yields an activation energy of 14.4 ± 0.7 kJ/mol, which is quite close to the $Q_{P(tr)}$ values (18.0 to 22.5 kJ/mol) of cold worked Au, but is much less than the energy of migration of monovacancies

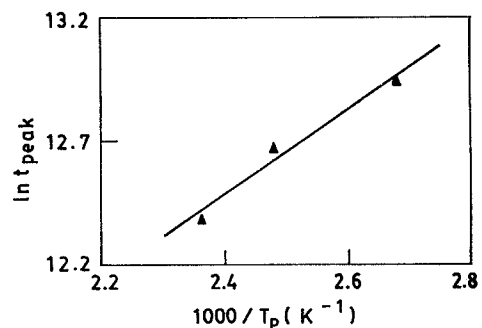


Fig. 6. Variation of t_{Peak} as a function of T_P .

(80.6 kJ/mol) or divacancies (68.16 kJ/mol) in Au lattice [50,51]. It is known that excess vacancies created during cold working anneal out through the defects like grain boundaries, and the degree of localization or identity associated with such grain boundary vacancies will depend on the boundary type, boundary site and the interatomic forces, i.e., the metal in question [40,52]. Since a neutral radon atom occupies ~ 3 times the volume of the gold ion, the ^{222}Rn atom in the grain boundary may prefer to be associated with some particular size of the grain boundary vacancy cluster to promote its permeation. This conforms to the earlier proposition of Rimmer and Cottrell [13] that fission gases capture vacancies and permeate through grain boundaries.

5. Conclusion

The Permeability of ^{222}Rn in annealed and cold worked polycrystalline Au at $T_H \leq 0.32$ is strongly dependent on the thermal schedule in the course of permeation. Virgin polycrystalline annealed Au remains impermeable to ^{222}Rn during prolonged (4.5–35 d) isothermal holding at 30, 100 and 150°C, but the permeation is triggered when Au is subjected to a thermal cycle of negative magnitude, and the effect can not be attributed to the rupture of any surface layer. Probably, here the lattice strain around large ^{222}Rn atoms in the presence of the thermal gradient may play a significant role.

In annealed Au, permeability gradually increases to a plateau, $N_{\text{Rn(steady)}}$ during prolonged isothermal holding (> 160 h), and $N_{\text{Rn(steady)}}$ increases with the increase in holding temperature. The $Q_{\text{P(tr)}}$ values determined by step heating experiments of short duration (~ 12 h) varied between 33.2 to 35.4 kJ/mol, which agrees well with $Q_{\text{P(st)}} \approx 34.6$ kJ/mol derived from permeation plateaux in prolonged isothermal holding (> 160 h), indicating identical mechanism of permeation operative in both types of treatments. The small magnitude of N_{Rn} (e.g., ≈ 0.7 atoms/mm² s) and the unusually low values of $Q_{\text{P(tr)}}$ or $Q_{\text{P(st)}}$ possibly indicate that ^{222}Rn permeates in annealed Au through some defects like grain boundaries or grain boundary triple points.

Virgin cold worked polycrystalline Au is permeable to ^{222}Rn at room temperature. Here the $Q_{\text{P(tr)}}$ values (18.0 to 22.5 kJ/mol) are smaller and N_{Rn} is about two orders of magnitude higher than those of annealed Au, which may be attributed to the structural changes in diffusion paths (e.g., grain boundaries) by deformation induced defects. Relaxation of some structural defects in cold worked Au was evident during permeation at $T_H < 0.28$. Here, prolonged isothermal holding at any T_P results in a permeation peak that seems to be associated with a very small activation energy of 14.4 kJ/mol. Probably, ^{222}Rn atoms residing in the defects like grain boundaries interact with excess vacancies to promote its permeation.

Acknowledgements

The work is sponsored by the Department of Atomic Energy, Government of India, vide grant Nos. 34/7/89-G and 34/4/95-R&D-II/678. The authors are thankful to Dr R.P. Sharma, Dr Srikumar Banerjee, and Dr G. Venkataraman for stimulating discussions and constant encouragement.

References

- [1] A.D. LeClaire, Diffus. Defect Data 33 (1983) 1.
- [2] A.D. LeClaire, Diffus. Defect Data 34 (1983) 1.
- [3] H.H. Johnson, Metall. Trans. A19 (1988) 2371.
- [4] G.M. Pressouyre, Acta Metall. 28 (1980) 895.
- [5] M.M. Makhlof and R.D. Sission Jr., Metall. Trans. A22 (1991) 1001.
- [6] M.A. Futterer, X. Raepsaet and E. Proust, Fusion Eng. Des. 29 (1995) 225.
- [7] N.M. Ghoniem, Res. Mech. 4 (1984) 287.
- [8] A.M. Hassanein and D.K. Sze, Fusion Technol. 10 (1986) 1355.
- [9] V. Philips, K. Sonnenberg and J.M. Williams, J. Nucl. Mater. 107 (1982) 271.
- [10] D.B. Bullen, Diss. Abstr. Int. 45 (1984) 219.
- [11] W.D. Urey, J. Am. Chem. Soc. 55 (1933) 3242.
- [12] C.J. Smithells and C.E. Ransley, Proc. R. Soc. A150 (1935) 172.
- [13] D.E. Rimmer and A.H. Cottrell, Philos. Mag. 2 (1957) 1345.
- [14] H.J. Matzke, G. Rickers and G. Sorensen, Acta Metall. 20 (1972) 1241.
- [15] Y. Legoux and J. Merini, J. Less Common Met. 105 (1985) 169.
- [16] S.K. Pabi and H. Hahn, J. Phys. Chem. Solids 49 (1988) 1035.
- [17] S.K. Bhattacharyya and S.K. Pabi, Diffus. Defect Forum 138&139 (1996) 63.
- [18] M. Hashimoto and R.M. Latanisi, Acta Metall. 36 (1988) 1837.
- [19] W.Y. Choo and J.Y. Lee, Metall. Trans. A14 (1983) 1299.
- [20] B.G. Pound, Acta Metall. Mater. 39 (1991) 2099.
- [21] Metals Hand Book, Vol. 9, Metallography and Microstructures (American Society for Metals, Metals Park, OH, 1985) pp. 1–19.
- [22] W. Seelmann-Eggebert, G. Pfenning and H. Munzel, Karlsruhe Nuklidkarte (Gesellschaft für Kernforschung, Karlsruhe, 1974).
- [23] F. Ajzenberg-Selove, Nuclear Spectroscopy, Part A (Academic Press, New York, 1960) p. 194.
- [24] H.J. von den Driesch and P. Jung, High Temp. High Pressures 12 (1980) 635.
- [25] G.N. Johnson, Philos. Mag. 6 (1961) 943.
- [26] F.G. Hewitt, J.A. Lacey and E. Lyall, React. Technol. 1 (1960) 167.
- [27] Lange's Handbook of Chemistry, 13th Ed. (McGraw-Hill, New York, 1985) pp. 3–121.
- [28] R. Birringer, U. Herr and H. Gleiter, Trans. Jpn. Inst. Met. Suppl. 27 (1986) 43.
- [29] R. Birringer, Mater. Sci. Eng. A117 (1989) 33.

- [30] G. Rickers and G. Sorensen, *Phys. Status Solidi* 32 (1969) 597.
- [31] H.M. Gilder and D. Lazarus, *J. Phys. Chem. Solids* 26 (1965) 2081.
- [32] G. Martin and B. Perrailon, *J. Phys. Colloq.* C4(36) (1975) 165.
- [33] J.M. Tobin, *Acta Metall.* 5 (1957) 398.
- [34] J.M. Tobin, *Acta Metall.* 7 (1959) 701.
- [35] D. Turnbull, *Phys. Rev.* 76 (1949) 471.
- [36] R.E. Hoffman and D. Turnbull, *J. Appl. Phys.* 22 (1951) 634.
- [37] A.D. LeClaire and A.H. Rowe, *Rev. Metall. Paris* 52 (1955) 94.
- [38] H.J. Matzke, G. Rickers and G. Sorensens, *Acta Metall.* 23 (1975) 1529.
- [39] M.W. Grabski and R. Korski, *Philos. Mag.* 22 (1970) 707.
- [40] H. Gleiter, *Mater. Sci. Eng.* 52 (1982) 91.
- [41] H.J. Hofler, H. Hahn and R.S. Averback, *Atomic Migration and Defects in Materials* (Sci-Tech Publications, Liechtenstein, 1991) pp. 195–210.
- [42] R.W. Cahn, *Physical Metallurgy, Part II* (North-Holland, New York, 1983) pp. 1595–1671.
- [43] F.R.N. Nabarro, *J. Inst. Met.* 66 (1940) 312.
- [44] W. Koster and F. Sperner, *Z. Metallkd.* 44 (1953) 217.
- [45] C. Panseri and T. Federighi, *Acta Metall.* 8 (1960) 217.
- [46] P. Wilkes, *Acta Metall.* 16 (1968) 863.
- [47] N.F. Mott, *J. Inst. Met.* 60 (1937) 267.
- [48] S.K. Pabi and A.K. Mallik, *Mater. Sci. Eng.* 21 (1975) 149.
- [49] I. Manna and S.K. Pabi, *J. Mater. Sci. Lett.* 7 (1988) 1299.
- [50] R.W. Balluffi and R.W. Siegel, *Lattice Defects in Quenched Metals* (Academic Press, New York, 1965) pp. 694–708.
- [51] J.A. Ytterhus, R.W. Siegel, and R.W. Balluffi, *Lattice Defects in Quenched Metals* (Academic Press, New York, 1965) pp. 679–691.
- [52] W. Hahn and H. Gleiter, *Acta Metall.* 29 (1981) 601.